



SRTTU

Journal of Computational and Applied Research
in Mechanical Engineering

jcarme.sru.ac.ir

JCARME

ISSN: 2228-7922

Research paper

Fracture analysis of pre-cracked and notched thin plates using peridynamic theory

L. Abbasiniyan, S. H. Hoseini and S. Faroughi*

Faculty of Mechanical Engineering, Urmia University of Technology, Urmia, Iran

Article info:

Article history:

Received: 23/04/2019

Revised: 22/08/2019

Accepted: 25/08/2019

Online: 28/08/2019

Keywords:

Peridynamic theory,

Brittle fracture,

Crack branching,

Thin plate.

*Corresponding author:

sh.faroughi@uut.ac.ir

Abstract

In this paper, the crack propagation and branching in the pre-cracked and notched samples have been modeled using nonlocal peridynamic theory. The bond-based peridynamic model has been numerically implemented which make it possible to simulate various features of dynamic brittle fracture such as crack propagation, asymmetries of crack paths and successive branching. The fracture simulation of thin plates made of a brittle material with different crack and notch patterns has been considered. The molecular dynamics open-source free LAMMPS code has been updated to implement the peridynamic theory based modeling tool for two-dimensional numerical analysis. The simulations show that, the simulation time significantly decreases which is the core and distracting deficiency of the peridynamic method. Moreover, the simulated results demonstrate the capability of peridynamic theory to precisely predict the crack propagation paths as well as crack branching during dynamic fracture process. The good agreement between simulation and experiments is achieved.

1. Introduction

The peridynamic theory has been developed to introduce a new framework that unites the modeling of continuous media and discontinuities within it. The mathematical description of a solid in classical continuum mechanics depends on partial differential equations (PDEs). The classical theory has provided a reasonable approximation to the response of materials in macro-scale. However, at smaller scales, micro-scales and even interatomic dimensions, it is essential to

introduce a new description to include the modeling of discrete particles and to allow the explicit modeling of nonlocal forces known to effect the behavior of real materials [1]. Similar considerations should be applied to cracks and other discontinuities [2-4]. The PDEs of the classical continuum mechanics theory do not apply directly on a crack or dislocation because the deformation is discontinuous. In peridynamic theory, the PDEs of the classical theory of continuum mechanics has been replaced with integral or integro-differential equations [5]. These equations are based on a

model of internal forces in which material points interact with each other straightly over finite distances. The peridynamic theory evaluates the discontinuities according to the same field equations as for continuous deformation [6]. It also has the treats discrete particles according to the same field equations as for continuous media. The ability to treat both the nano-scale and the macro-scale within the same mathematical framework makes the peridynamic theory an interesting method to simulate the multi-scale real material.

The peridynamic theory was first introduced by Silling [7] and Silling et al. [8]. They replaced the derivatives in classical mechanics with integral equations and reformulate the equation of motion. The governing equations in the proposed model are developed based on the concept of continuity within a finite distance, horizon, and an internal forces model in body, in which the material points (particles) directly exert force on each other. Ni et al. [9] using two new implicit solution algorithms have introduced the static analysis of crack propagation problems. They have discretized structures via an efficient coupled FEM-PD approach and compared the results with linear analysis. Silling and Askari [10] presented a meshless method based on peridynamics theory to find a numerical solution for dynamics problems. They also investigated the stability and accuracy of this method used to model the dynamic brittle crack growth. Kilic and Madenci [11] studied the failure and stability of structures using peridynamics theory. They examined rectangular columns and plates under pressure and temperature loading to determine the buckling properties of peridynamics problems. Ha and Bobaru [12-14] modeled the dynamic crack growth and found the characteristics of dynamic brittle fracture using peridynamics theory. They also examined the effective parameters involved in crack branching, secondary cracks and instability of crack paths. A new peridynamics approach has been proposed by Ren et al. [15] which introduces a dual-horizon concept. In that framework, the new method to examine crack growth based on the dual-horizon peridynamics approach was introduced and the obtained results have been compared with the bond-based peridynamics theory. The validity and stability of a peridynamic model is evaluated by Zhang et al. for fatigue cracking in

homogeneous and composite materials [16]. Peridynamics theory has also been used for modeling of delamination growth [17] and damage growth prediction in center-cracked fiber reinforced composite laminates [18]. Consequently, Yu et al. [19] modeled progressive damage, fracture and delamination in fiber reinforced composite laminates under a tensile load with a notch or open hole. Madenci et al. [20] have predicted the unguided crack paths propagation in isotropic materials under complex loads using peridynamics. Problems of crack growth in a 4-point shear specimen and a compact tension test with a sink and a miss-hole with a pre-existing crack under mixed-mode loading conditions are considered in their analysis. Littlewood et al. [21] applied modal analysis with state-based peridynamics to identify characteristic frequency shifts caused by structural damage evolution for a simply-supported beam problem. They compared the results of peridynamics against the classical analytic solution for the first five structural modes. Qian et al. [22] introduced a damage analysis model based on a unified cubic lattice for peridynamics formulation of an I-beam under fixed and impact loads. They concluded that for materials containing defects e.g., cracks and pores, two key modeling parameters i.e., near-field region radius and m-value have a significant effect on the path and direction of crack propagation. Silling et al. [23] have proposed a condition for the appearance of a discontinuity in a loaded peridynamic solid leading to a material stability condition for the spontaneous nucleation of a crack. The stable crack growth process in an elastic plate under uniaxial tension was studied based on the strain energy density criterion. Dong and et al [24] presented a new model based on material properties and bond-based peridynamic to predicted mode-I crack propagation. Rokkam et al. [25] presented a novel micro-chemically sensitive peridynamics approach to model corrosion damage, corrosion pitting, nucleation, crack propagation and branching phenomena under synergistic effects of corrosion and mechanical loading. Ni et al. [26] used a very efficient coupled FEM-OSB-PD (ordinary state-based peridynamics) method for modeling a complex 3D crack propagation problem in brittle materials. The method unifies both advantages of classical mechanics efficiency and peridynamics flexibility. The adaptive

dynamic relaxation approach is also used in their analysis as the numerical solution. In this research, it has been attempted to investigate the crack growth on thin plates with different crack patterns based on the peridynamic theory. The main goal of this study is to implement the bond-based peridynamic method in a molecular dynamic code to decrease the computational time. Therefore, the peridynamic method has been numerically implemented in the open source LAMMPS code. LAMMPS is a molecular dynamics code that has been developed by Sandia National Laboratories [27]. The bond based peridynamic model is widely used in literature to describe the fracture behavior of material. This model precisely predict the material behavior up to fracture especially for brittle material. The pre-cracked and notched thin plates made of a brittle material were simulated in LAMMPS and the crack propagation and branching were considered during brittle fracture process.

2. Peridynamic theory

The peridynamic theory implemented the integration of nodal forces rather than the differential form of the equations of motion [28]. Therefore, problems like material discontinuities in the classical formulation are omitted. Naturally, peridynamics is a nonlocal formulation whose material points are distributed by a spatial distance interrelated with each other. The bond-based peridynamic formulation of the equation of motion at a point \mathbf{x} and time t is [10]

$$\rho(\mathbf{x})\ddot{\mathbf{u}}(\mathbf{x}, t) = \int_{\mathcal{H}_x} \mathbf{f}(\mathbf{u}(\mathbf{x}', t) - \mathbf{u}(\mathbf{x}, t), \mathbf{x}' - \mathbf{x})dV_{x'} + \mathbf{b}(\mathbf{x}, t) \quad (1)$$

where $\ddot{\mathbf{u}}$ designates the acceleration vector, \mathbf{u} denotes the displacement vector, \mathbf{b} is the applied body force, and ρ is the density. In addition, \mathbf{f} is the pairwise force function which is the force per volume squared that the point \mathbf{x}' exerts on the point \mathbf{x} . Points \mathbf{x} and \mathbf{x}' that are separated by a distance greater than certain distance δ which called the horizon, do not interact in the material model applied at either points. The horizon size generally is the characteristic size of the nonlocal interaction. Material within the horizon of \mathbf{x} is called the

family of \mathbf{x} , denoted \mathcal{H}_x , in Fig. 1. The relative position vector in the reference configuration, ξ , is called a bond and the relative displacement vector is designated as η .

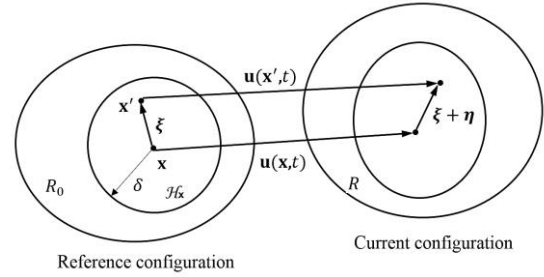


Fig. 1. The deformation of a point and its family based on peridynamic concept.

The balance of the linear momentum and angular momentum in the bond-based peridynamic would be defined as the following relations

$$\begin{aligned} \mathbf{f}(\xi, \eta) &= -\mathbf{f}(-\xi, -\eta), \quad \forall \xi, \eta \\ (\xi + \eta) \times \mathbf{f}(\xi, \eta) &= 0, \quad \forall \xi, \eta \end{aligned} \quad (2)$$

According to Eq. (2), the forces that two points exert on each other are identical in norm with opposite direction. Furthermore, these forces coincide with the relative position vector in the current configuration. For a micro-elastic material introduced by Silling [7], the pairwise force function is derived from a scalar-valued function called the micro-elastic potential function:

$$\mathbf{f}(\xi, \eta) = \frac{\partial w(\xi, \eta)}{\partial \eta} \quad (3)$$

Silling and Askari [10] suggested a prototype microelastic brittle (PMB) material with the following pairwise force function:

$$\mathbf{f}(\xi, \eta) = c(\xi)s(\xi, \eta) \frac{\xi + \eta}{\|\xi + \eta\|} \quad (4)$$

where c is the bond stiffness called the micromodulus and s is the relative elongation of a bond defined as

$$s(\xi, \eta) = \frac{\|\xi + \eta\| - \|\xi\|}{\|\xi\|} \quad (5)$$

The relation between the micromodulus and the isotropic elastic constants is determined by the comparison between the strain energy density

obtained from the peridynamic theory and the strain energy density obtained from the classical theory of elasticity for the same loading condition. For a microelastic material, the strain energy density at a point is the integral of the micropotential over its horizon. For a point with a horizon located far from surfaces or interfaces, the strain energy is defined as [10]:

$$W = \frac{1}{2} \int_{\mathcal{H}_{x'}} w(\xi, \eta) dV_{x'} \quad (6)$$

For the prototype microelastic brittle (PMB) material the micropotential function is:

$$w(\xi, \eta) = \frac{1}{2} c s^2 \|\xi\| \quad (7)$$

Equaling the density of strain energy in peridynamic formulation with the classical continuum one under the plane stress condition, the micro-modulus is achieved as:

$$c = \frac{6E}{\pi \delta^3 (1-\nu)} \quad (8)$$

where E is the classical elastic Young's modulus and ν is the Poisson ratio. In the bond-based formulation of peridynamics theory, the Poisson ratio is constant for all materials and is 1/4 for an isotropic and linear micro-elastic material.

The micro-moduli is estimated for material points inside the body far from the boundary, at least equivalents to a horizon. The micro-modulus for points closes to boundary is greater than other places. It is because the integration is done over a reduced domain. In this paper, the micro-modulus for the points adjacent to the boundary is assumed to be equal to that for points inside the body. This makes a 'softer' material near the boundary which is called the peridynamic 'skin effect'. However, with decreasing the size of horizon, the skin effect becomes negligible.

In the bond-based formulation of peridynamics theory, it is assumed that the material points are connected through bonds and each bond could endure a special elongation value, s_0 . A bond disrupts when its elongation is greater than this critical value. This special value is usually termed the critical relative elongation parameter in literature. Once a bond disrupts, it remains broken forever. Based on this idea, the deformation of a microelastic material in peridynamic formulation is generally history-

dependent. The 'critical relative elongation parameter 'may be calculated using the concepts of fracture mechanics.

Rupture of a body into two portions across a fracture plane includes breaking all the bonds that linked points in the opposite surfaces. The energy per unit fracture length for the rapture of the body into two portions is the fracture energy, G_0 . In 2D, the relation between the 'critical relative elongation 'and the critical fracture energy is [29]:

$$G_0 = 2 \int_0^\delta \int_z^\delta \int_0^{\frac{\cos^{-1} z}{\|\xi\|}} \left(\frac{c s_0^2 \|\xi\|}{2} \right) \|\xi\| d\theta d\|\xi\| dz \quad (9)$$

For the constant micromodulus, Eq. (8), it can be calculated:

$$s_0 = \sqrt{\frac{4\pi G_0}{9E\delta}} \quad (10)$$

implementing a constant 'critical relative elongation 'causes weaker material in places where previously disruption occurred. This is completely similar to the skin effect whose integration to compute G_0 , Eq. (9) is done on a smaller area in the broken region or near the boundary. If the same G_0 is implemented everywhere, that would make a larger 'critical relative elongation 'for points in the broken region or near the boundary. Without any modification of 'critical relative elongation , the material becomes weaker in front of the crack-tip than other parts of the material. In this paper the modification proposed by Silling and Askari [10] is applied on 'critical relative elongation. According to this modification, the critical relative elongation is defined as:

$$s_0 = s_{00} - \alpha s_{min}, \quad s_{min} = \min \left\{ \frac{\|\xi+\eta\| - \|\xi\|}{\|\xi\|} \right\} \quad (11)$$

Where s_{00} and α are constants, with α typically on the order of 1/4. In Eq. (11), the critical relative elongation depends on s_{min} , the current minimum stretch among all bonds are connected to a given material point.

3. Simulation procedure and results

Numerical simulations are effective tools for understanding physical phenomena as well as laboratory experiments. One of the effective

methods to simulate the material behavior in the micro and nano scales is molecular dynamics. The free open source LAMMPS software is one of the more accurate molecular dynamics program from Sandia National Laboratories. LAMMPS is generally a classical molecular dynamics code focusing on materials behavior modeling. LAMMPS has potential to simulate the solid-state materials, soft matter and coarse-grained or mesoscopic systems. It can be used to model atoms or, more generically, as a parallel particle simulator at the atomic, meso, or continuum scale. In this software, each point of the peridynamic model is assumed to be an atom. At first, a regular pattern of points based on the geometry of component is established and the neighborhood of each point is determined. Then, between each point and other point in its family, a bond is defined. After defining the location of each point, the initial velocity and displacement of each point is applied and the solution is divided to finite time steps. After calculating the interaction force between each point in terms of potential functions and applying simulation conditions, based on the integral form of equation of motion the new location and velocity of points are estimated in each step. This loop is repeated for all time steps, and consequently the obtained values are saved in the code outputs. As mentioned before, force between each point is obtained from potential function. Definition of the potential function is the main part of the simulation. This function is defined for interactions between N points as follows:

$$\phi(r) = \sum_i \phi_1(r_i) + \sum_i \sum_{j>i} \phi_2(r_i, r_j) \quad (12)$$

Where r is the location vector from the center of points and ϕ_1 is the effect of external field and ϕ_2 is the interaction between a pair of points. In the peridynamic model, the distance between neighborhood points and the size of horizon, δ , should be determined. In this work, the distance between each pair of points assumes $\Delta x = 0.0005 m$ and the size of horizon is $\delta \cong 4\Delta x$. When the horizon set $\delta \cong 4\Delta x$, the sufficient particles locate in the horizon, more than 32 particles in 2D simulation. The values of parameters (c, s, δ and α) can be calculated based on the mechanical properties of the material. s and α are used as a bond breaking criteria, and in this work α is assumed to be 0.02 which is

proposed by Silling and Askari [10]. In each time step, the elongation of every bonds are calculated and compared with the critical value. If the elongation of bonds exceeds the critical values, then the bond would be assumed broken and permanently deleted from the model. The flowchart of the simulation procedure is presented in Fig. 2.

In the present study, the propagation of crack in four sample plates containing pre-crack has been investigated. Duran 50 glass, a brittle material, used in simulations. DURAN is a brand name for the borosilicate glass 3.3 (DIN ISO 3585) manufactured by the German company DURAN Group [30].

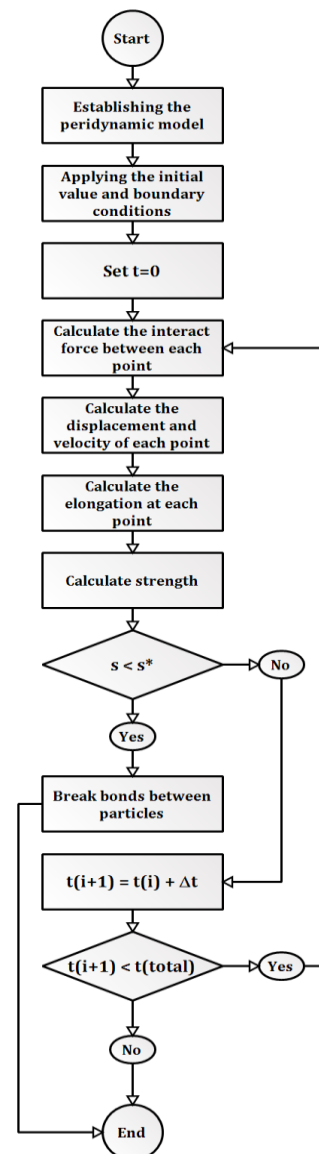


Fig. 2. Schematic diagram for parallel implementations PMB Peridynamics model.

Because of its high resistance to heat and temperature variations, as well as its high mechanical strength and low coefficient of expansion, DURAN is used for laboratory devices, cathode ray tubes, transmitting tubes, and speculums. The mechanical properties of this material are presented in Table. 1.

Where E is Young's modulus, ν is the Poisson ratio, ρ is density and G_0 is the critical energy release rate. In the bond-based peridynamic, the Poisson ratio is a constant value equals 0.25. For the brittle materials this value is reasonable but for ductile ones the other type of peridynamic models should be implemented. The first sample plate is a rectangular plate with single edge long crack in tension, Fig. 3. The uniform normal stress is applied to the two edges of the plate perpendicular to the crack. In the simulations, the effect of the applied force on the crack propagation behavior is considered. Initially, the horizon size is set 0.002m and uniform tensile stress $\sigma=12$ MPa is applied. In comparison with plate geometries, the horizon size is set 0.002m to guarantee the convergence of the results. For horizon size smaller than 0.002m the results do not change. Moreover, the applied load is selected to ensure that the fracture occurs.

Peridynamic simulation predicts a symmetrical crack path with simple branching, Fig. 4(a). As it can be seen in Fig. 4(b), this result coincides with the experiments reported by Ha and Bobaru [31]. The results were captured at $32\mu s$. These results demonstrate that the peridynamic method could precisely predict the material behavior up to fracture.

With increasing the applied force, the probability of severe crack branching is enhanced. In Fig. 5, the applied load on the first sample plate is increased up to $\sigma = 24$ MPa. As it can be seen, increasing the applied load causes secondary crack branching. This result is confirmed by experiments. In the simulation, the secondary crack branching is symmetric, but the experimental results show different results. The discrepancy between simulation and experiments come from the microscale anisotropy and heterogeneous behavior of the material. In this work, the material behavior is assumed to be homogeneous and isotropic. Further investigations on secondary crack branching will be conducted in the future work.

The second sample plate is a rectangular center-cracked plate. The geometry of this plate is depicted in Fig. 6. The uniform stress is applied to the two edges of the plate perpendicular to the crack direction.

In the simulation, the applied stress is 1.45 Mpa. Fig. 7 shows the crack propagation paths. The crack path is perpendicular to the applied load direction and no crack branching is observed inside the plate. However, the branching phenomena occurs near the edges. The crack propagates symmetrically in the path parallel to the initial crack direction. Moreover, the branching near the edges happens symmetrically.

The third sample plate is a rectangular plate containing a circular hole subjected to uniform remote stress. No pre-cracked is defined in this model. The configuration of this plate is illustrated in Fig. 8.

Table 1. Values of the model parameters.

Material	ρ	E(GPa)	ν	$G_0(J/m^2)$
Duran 50 glass	2235	65	0.2	204

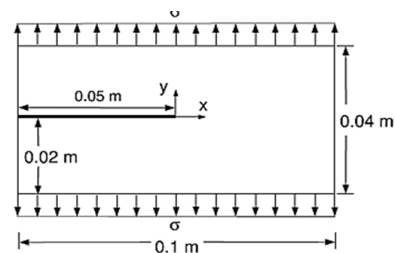


Fig. 3. Configuration of the first sample plate.

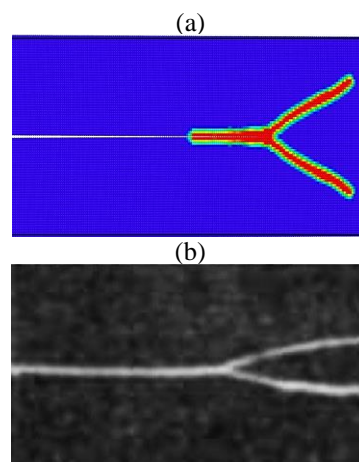


Fig. 4. (a) Crack propagation in the first sample plate with the horizon size and applied stress equal 0.002m and $\sigma=12$ MPa, respectively; (b) Experimental result.

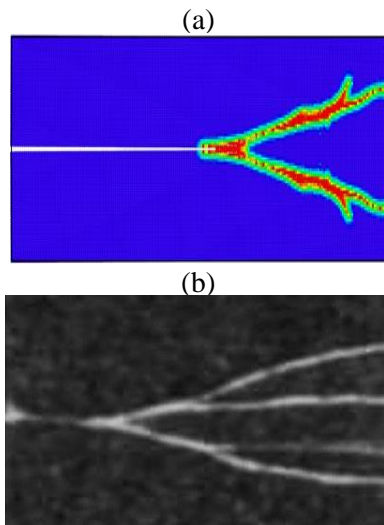


Fig. 5. (a) Crack propagation in the first sample plate with the horizon size and applied stress equal 0.002m and $\sigma=24$ MPa, respectively; (b) Experimental result.

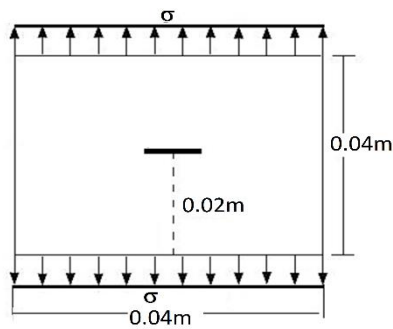


Fig. 6. Geometry of the second sample plate.

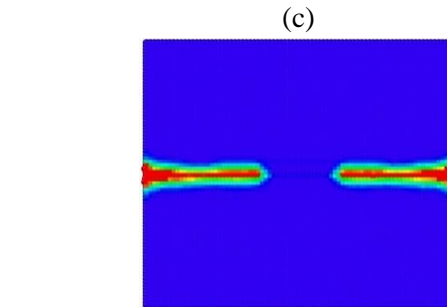
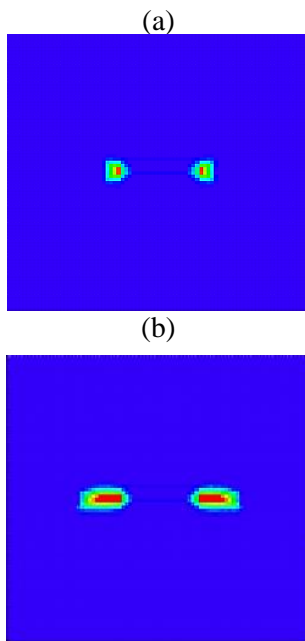


Fig. 7. Crack paths in second plate sample (a) at $t=6\mu s$, (b) at $t=13\mu s$ and (c) at $t=28\mu s$.

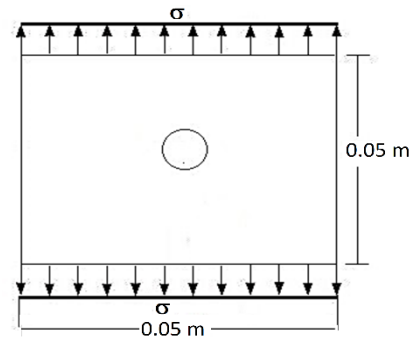


Fig. 8. Configuration of the third sample plate.

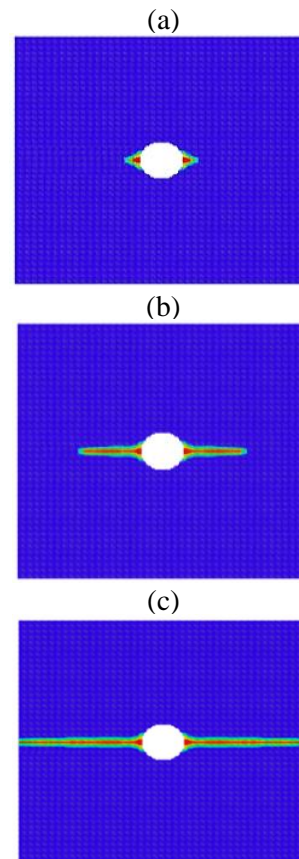


Fig. 9. Crack paths in third plate sample at (a) $t = 10\mu s$, (b) $t = 40\mu s$, and (c) $t = 90\mu s$.

The purpose of this simulation is to examine the effect of the stress concentration on the crack growth path. The external load equals $\sigma=10.5$ Mpa is applied to the two edges of the plate. As it can be seen in Fig. 9, the crack initiates from the hole and grows symmetrically to the edges.

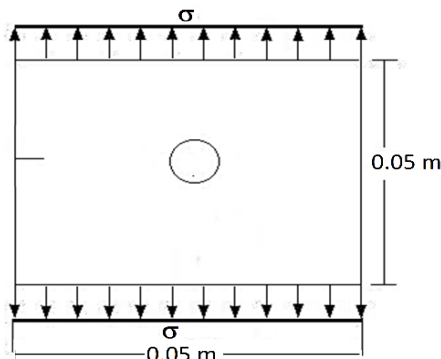


Fig. 10. Geometry of a fourth sample plate.

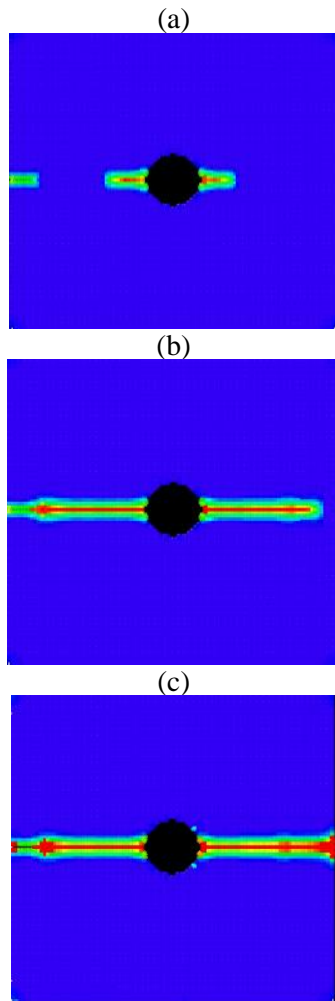


Fig. 11. Crack paths in fourth plate sample (a) $t=34$, (b) $t= 42 \mu s$, (c) $t= 60 \mu s$.

It is predictable that the crack initiation occurs near a location with the maximum stress due to the stress concentration. In this sample plate, the crack propagates without branching. The fourth, and the last sample plate is a rectangular plate containing a circular hole and a single edge crack subjected to uniform remote stress. The shape of this plate is shown in Fig. 10.

This simulation examines the effect of the stress concentration on the crack growth path when a pre-crack exists. The external load is $\sigma=25.5$ Mpa. The length of the crack is chosen in such a way that the stress around the crack and hole does not influence each other. As it can be seen in Fig. 11, cracks initiate from the hole and concurrently the edge crack grows into the plate. All cracks propagate in the path perpendicular to the loading direction. Finally, the cracks join together and divide the plate into two parts. In the fourth sample plate, the crack also propagates without branching.

4. Conclusions

In this paper the fracture analysis and crack propagation in the pre-cracked and notched thin plates using bond-based peridynamic theory have been considered. The method has been numerically implemented in the open source LAAMPS code. LAMMPS is a molecular dynamics code. In this work, the LAMMPS code has been updated to implement the peridynamic method. This significantly decreases the simulations time which is the core deficiency of the peridynamic method. The pre-cracked and notched thin plate made of a brittle material were simulated in LAMMPS and the crack propagation and branching considered during the brittle fracture process.

The simulated results show that the peridynamic theory is a powerful method to simulate the fracture processes. The simulation of the four sample plates with different crack and notch patterns confirms that this nonlocal method could precisely predict the crack propagation path as well as crack branching. It should be mentioned that the disadvantage of the peridynamic method which is the computational time consuming is depressed.

References

- [1] S. R. Chowdhury, M. M. Rahaman, D. Roy and N. Sundaram, "A micropolar peridynamic theory in linear elasticity", *Int. J. Solids Struct.*, Vol. 59, pp.171-182, (2015).
- [2] A. C. Eringen, *Continuum Physics: Polar and Nonlocal Field Theories*, first ed., Elsevier, (1976).
- [3] A. C. Eringen, *Continuum Physics: Mixtures and EM Field Theories*, first ed., Elsevier, (1976).
- [4] K. Khorshidi and A. Fallah, "Buckling analysis of functionally graded rectangular nano-plate based on nonlocal exponential shear deformation theory", *Int. J. Mech. Sci.*, Vol. 113, pp. 94-104, (2016).
- [5] S. A. Silling and R. B. Lehoucq, "Peridynamic theory of solid mechanics", *Adv. Appl. Mech.*, Vol. 44, pp. 73-168, (2010).
- [6] A. Ahadi and S. Melin, "Capturing nanoscale effects by peridynamics", *Mech. Adv. Mater. Struct.*, Vol. 25, No. 13, pp. 1115-1120, (2018).
- [7] S. A. Silling, "Reformulation of elasticity theory for discontinuities and long-range forces", *J. Mech. Phys. Solids*, Vol. 48, No. 1, pp. 175-209, (2000).
- [8] S. A. Silling, M. Epton, O. Weckner, J. Xu and E. Askari, "Peridynamic states and constitutive modeling", *J. Elast.*, Vol. 88, No. 2, pp. 151-184, (2007).
- [9] T. Ni, M. Zaccariotto, Q. Z. Zhu and U. Galvanetto, "Static solution of crack propagation problems in Peridynamics", *Comput. Methods Appl. Mech. Eng.*, Vol. 346, pp.126-151, (2019).
- [10] S. A. Silling and E. Askari, "A meshfree method based on the peridynamic model of solid mechanics", *Comput. Struct.*, Vol. 83, No. 17-18, pp. 1526-1535, (2005).
- [11] B. Kilic and E. Madenci, "Structural stability and failure analysis using peridynamic theory", *International J. Non-Linear Mech.*, Vol. 44, No. 8, pp. 845-854, (2009).
- [12] Y. D. Ha and F. Bobaru, "Studies of dynamic crack propagation and crack branching with peridynamics", *Int. J. Fract.*, Vol. 162, No. 1, pp. 229-244, (2010).
- [13] F. Bobaru and Y. D. Ha, "Adaptive refinement and multiscale modeling in 2D peridynamics", *Int. J. Multiscale Comput. Eng.*, Vol. 9, No. 6, pp. 635-660, (2011).
- [14] Y. D. Ha and F. Bobaru, "Characteristics of dynamic brittle fracture captured with peridynamics", *Eng. Fract. Mech.*, Vol. 78, No. 6, pp. 1156-1168, (2011).
- [15] H. Ren, X. Zhuang, Y. Cai and T. Rabczuk, "Dual-horizon peridynamics", *Int. J. Numer. Methods Eng.*, Vol. 108, No. 12, pp. 1451-1476, (2016).
- [16] F. Bobaru and G. Zhang, "Why do cracks branch? A peridynamic investigation of dynamic brittle fracture", *Int. J. Fract.*, Vol. 196, No. 1-2, pp. 59-98, (2015).
- [17] Y. L. Hu, N. V. De Carvalho and E. Madenci, "Peridynamic modeling of delamination growth in composite laminates", *Compos. Struct.*, Vol. 132, pp. 610-620, (2015).
- [18] B. Kilic, A. Agwai and E. Madenci, "Peridynamic theory for progressive damage prediction in center-cracked composite laminates", *Compos. Struct.*, Vol. 90, pp. 141-151, (2009).
- [19] Y. Hu, Y. Yu and H. Wang, "Peridynamic analytical method for progressive damage in notched composite laminates", *Compos. Struct.*, Vol. 108, pp. 801-810, (2014).
- [20] E. Madenci, K. Colavito and N. Phan, "Peridynamics for unguided crack growth prediction under mixed-mode loading", *Eng. Fract. Mech.*, Vol. 167, pp. 34-44, (2016).
- [21] P. Seleson and D. Littlewood, "Convergence studies in meshfree peridynamic simulations" *Comput. Math. Appl.*, Vol. 71, No. 11, pp.2432-48, (2016).
- [22] Q. Du, Y. Tao and X. Tian, "A peridynamic model of fracture mechanics with bond-breaking", *J. Elast.*, Vol. 132, No. 2, pp. 197-218, (2018).

- [23] S. A. Silling, O. Weckner, E. Askari and F. Bobaru, “Crack nucleation in a peridynamic solid”, *Int. J. Fract.*, Vol. 162, No. 1, pp. 219–227, (2010).
- [24] D. Yang, W. Dong, X. Liu, S. Yi and X. He, “Investigation on mode-I crack propagation in concrete using bond-based peridynamics with a new damage model”, *Eng. Fract. Mech.*, Vol. 199, pp. 567-581, (2018).
- [25] S. Rokkam, M. Gunzburger, M. Brothers, N. Phan and K. Goel, “A Nonlocal Peridynamics Modeling Approach for Corrosion Damage and Crack Propagation”, *Theor. Appl. Fract. Mech.*, Vol. 101, pp. 373-387, (2019).
- [26] T. Ni, M. Zaccariotto, Q. Z. Zhu and U. Galvanetto, “Coupling of FEM and ordinary state-based peridynamics for brittle failure analysis in 3D”, *Mech. Adv. Mater. Struct.*, Vol. 28, No. 9, pp.875-890, (2021).
- [27] <https://www.sandia.gov/~sasilli/>
- [28] R. W. Macek and S. A. Silling, “Peridynamics via finite element analysis”, *Finite Elem. Anal. Des.*, Vol. 43, No. 15, pp. 1169-1178, (2007).
- [29] Y. D. Ha and F. Bobaru, “Studies of dynamic crack propagation and crack branching with peridynamics”, *Int. J. Fract.*, Vol. 162, No. 1-2, pp. 229-244, (2010).
- [30] E. Axinte, “Glasses as engineering materials: A review”, *Mater. Des.*, Vol. 32, No. 4, pp. 1717-1732, (2011).
- [31] Y. D. Ha and F. Bobaru, “Characteristics of dynamic brittle fracture captured with peridynamics”, *Eng. Fract. Mech.*, Vol. 78, No. 6, pp. 1156-1168, (2011).

Copyrights ©2021 The author(s). This is an open access article distributed under the terms of the Creative Commons Attribution (CC BY 4.0), which permits unrestricted use, distribution, and reproduction in any medium, as long as the original authors and source are cited. No permission is required from the authors or the publishers.



How to cite this paper:

L. Abbasiniyan, S. H. Hoseini and S. Faroughi, “Fracture analysis of pre-cracked and notched thin plates using peridynamic theory,”, *J. Comput. Appl. Res. Mech. Eng.*, Vol. 11, No. 2, pp. 329-338, (2022).

DOI: 10.22061/JCARME.2019.5136.1628

URL: https://jcarme.sru.ac.ir/?_action=showPDF&article=1135

